RSC Advances

ROYAL SOCIETY OF CHEMISTRY

www.rsc.org/advances

Journal Name

COMMUNICATION

Tuneable luminescence and morphology of amphiphilic platinum(II) complex via the incorporation of cationic surfactant

Received 00th January 20xx,
Accepted 00th January 20xx

DOI: 10.1039/x0xx00000x

www.rsc.org/

Xiaorui Zheng*[a, b], Haiyang Wang[a, b] and Yuan Li[a, b]

A new amphiphilic platinum(II) complex containing a quaternary ammonium group had been synthesized successfully. Of interest is that its monomer and excimer emission could be systematically controlled by the incorporation of a cationic surfactant, which led to a morphological transformation from fibers to ribbons then to sheets.

Supramolecular self-assembly, driven by various weak non-covalent interactions, provides an entry into a new class of materials with tunable structures and multiple functionalities.[1] In the past few decades, square-planar platinum(II) complexes have drawn more and more attention due to their intriguing spectroscopic and luminescence properties[2]. Meanwhile, square-planar platinum(II) complexes often tend to arrange themselves into oligomeric structures via Pt–Pt and/or π–π stacking interactions. Through controlling the above-mentioned intermolecular interactions, the spectroscopic and luminescence properties of platinum(II) complexes can be tuned purposively. Such aggregation-induced optical behaviors have resulted in many potential applications in the fields of chemical sensors and electro-optical devices.[2] However, stepwise tuneable optical outputs of platinum(II) complexes have only rarely been explored.[2l]

On the other hand, the assembly of surfactants has immense potential for the design of nanoscale architectures. For example, surfactants have been chosen as template to prepare hollow silica particles[3a]. Zhang et al.[3b] reported the facile organization of the inorganic sandwiched heteropolytungstomolybdate $K_{13}[Eu(SiW_9Mo_2O_{39})_2]$ into highly ordered supramolecular nanostructured materials by complexation with a series of cationic surfactants. Beaune et al.[3c] reported the fabrication of hybrid materials of magnetic and fluorescent vesicles based on surfactant. Fluorescence probes have been employed in structural investigations, such as fusion of surfactants vesicles[3d] and phase transitions. Besides, mixed surfactant solutions contain a variety of structures.[4] In the previous literature[4b], careful fluorescent probe investigation has shown that the phase behaviour of dodecyltrimethylammonium bromide (**DTAB**) didodecyldimethylammonium bromide (**DDAB**) mixtures is much richer than previously appreciated.

We herein reported an amphiphilic cationic platinum(II) complex (**$FPtNC_3$**) fabricated by linking (2-(4',6'-difluorophenyl)pyridinato-N,C2')(2,4-pentanedionato-O,O) (**FPt1**) with an ammonium salt group (Scheme 1). According to the previous reports[5], **FPt1** had a broad excimer emission and had been widely used in the field of white organic light emitting device as a single emissive dopant, in which the doping concentration was a key parameter to control the relative ratio of monomer and excimer emission. The ancillary ligand of the complex **$FPtNC_3$** was functionalized by a dodecyltrimethylammonium bromide (**DTAB**) group, which was a very advantageous self-assembling unit due to its strong hydrophobic interactions of alkyl chains in aqueous medium[4c-4f] and thus endowed the complex with an amphiphilic feature. Meanwhile, in order to control the luminescence of **$FPtNC_3$** efficiently, the cationic surfactant **DTAB** was added gradually into the aqueous solution of the complex. Interestingly, with the gradual addition of **DTAB**, the emission of **$FPtNC_3$** changed from weak-orange to bright-blue-green accompanied by a morphological transformation from fiber to ribbon then to sheet.

[a] *State Key Laboratory of Fluorine & Nitrogen Chemicals, Xi'an 710065, China;*
[b] *Xi'an Modern Chemistry Research Institute, Xi'an 710065, China; E-mail: zhxrui@qq.com*

Electronic Supplementary Information (ESI) available: Synthesis and characterization details of all compounds, additional Fluorescent micrograph, SEM and TEM images. See DOI: 10.1039/x0xx00000x

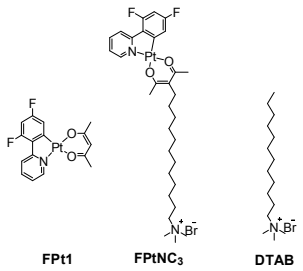

Scheme 1. Chemical structures of FPt1, $FPtNC_3$ and DTAB.

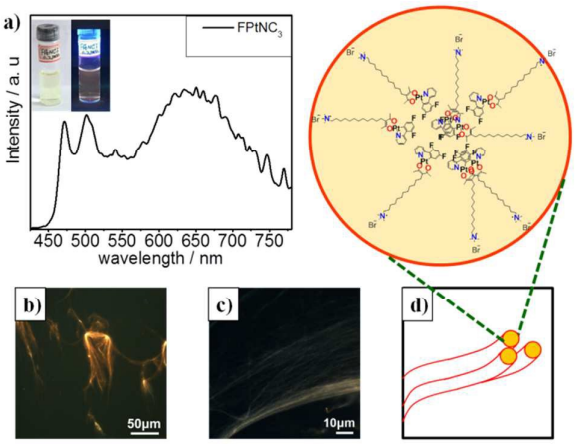

Fig. 1 (a) Emission spectra of $FPtNC_3$, the inner photographs show **$FPtNC_3$** under ambient light (left) and UV irradiation (right). (b,c) Fluorescent microscopic images of **$FPtNC_3$** aqueous solution. (d) Schematic representation of self-assemblied structure of **$FPtNC_3$**.

The platinum(II) complex **$FPtNC_3$** was synthesized according to the routine shown in Scheme S1 and fully characterized by ^1H and ^{13}C NMR spectra together with high-resolution electrospray ionization mass spectra (Fig. S1–S10). **$FPtNC_3$** was able to dissolve in organic solvents and water, confirming that the complex was amphiphilic. The resulting aqueous solution showed a yellowish color under ambient light and emitted weak orange light under UV irradiation (Fig. 1a, 0.2 mM). The UV-vis absorbance spectra (Fig. S12) and quantum yield (2%) measurements of **$FPtNC_3$** showed similar results with **FPt1** described in previous reports.[5c,5e]

Upon excitation at 385 nm, the aqueous solution showed four emission bands with comparable intensities, which were centered at 471 nm, 501 nm, 540 nm and 645 nm, respectively (Fig. 1a). According to the previous reports about **FPt1** and its analogues[5,6] the fore three bands originated from the monomer emission while the latter one the excimer emission. Fluorescence microscopic images showed that the complex **$FPtNC_3$** in water self-assembled into fibrous micelles with a length of several ten micrometers, which emitted weak orange light (Fig. 1c). After water evaporated, fibers disaggregated to form discrete fragment (Fig. S11).

According to previous studies of surfactants,[3,4] we deduced that the amphiphilic feature of **$FPtNC_3$** played an important role in its self-assembly. In water, as a result of the solvophobic effect, the complex formed the micelle and the hydrophilic ammonium salt groups were located on the outer side of the micelle. The hydrophobic core contained platinum(II) complex squares and alkyl chains. Inside of the hydrophobic core, the platinum(II) complexes were close enough to form the excimer. During the excitation process, the excimer received energy transferred from the monomer, resulting in luminescence quenching[6]. Due to the fact that the fraction of excimer was low and the energy transferred from the large part of monomers was not complete, the monomer emission and the broadband emission were observed (Fig. 1a). A possible model was presented in Fig. 1d, in which several fibrous micelles bonded together into a bigger volume fibrous aggregate.

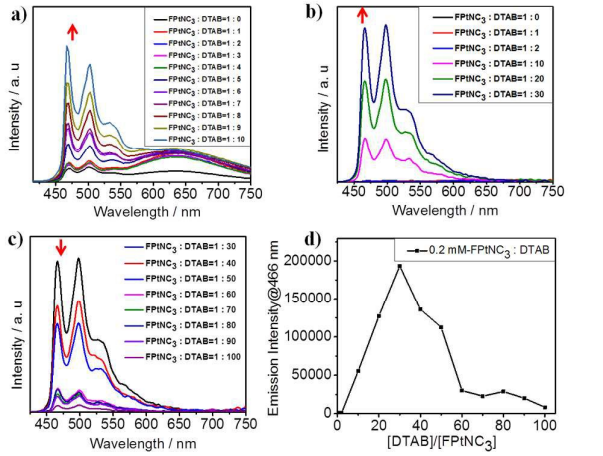

Fig. 2 Emission spectra of **$FPtNC_3$/DTAB** mixtures in water (λ_{exc}=385 nm). (a) Emission spectra of the mixtures at the molar ratio of 1:0–1:10. (b) Emission spectra of the mixtures at the molar ratio of 1:0 to 1:30. (c) Emission spectra of the mixtures at the molar ratio of 1:30 to 1:100. (d) Emission intensities of the mixtures at 466 nm.

To control energy transfer from the monomer efficiently, DTAB was added into the aqueous solution of **$FPtNC_3$**. A series of **$FPtNC_3$/DTAB** mixtures with different molar ratio (from 1:1 to 1:100, listed in Table S1) were prepared by adding the concentrated aqueous solution of **DTAB** to **$FPtNC_3$** solution. The original concentration of **$FPtNC_3$** was maintained at 0.2 mM. The concentrations of **$FPtNC_3$** in these mixtures decreased slightly while the total concentration of ammonium salt groups increased with the gradual addition of **DTAB**.

Upon UV irradiation at 365 nm, these **$FPtNC_3$/DTAB** mixtures indicated different emission from weak orange to bright blue-green with the increase of **DTAB** (Fig. S13). We thus investigated the optical properties of the above-mentioned mixtures through UV-vis absorption and luminescence measurements. When the molar ratio between **$FPtNC_3$** and **DTAB** ranged from 1:1 to 1:4, the monomer emission intensities of **$FPtNC_3$** in mixtures increased slightly (Fig. 2a). Comparatively, the excimer emission intensities enhanced obviously. After that, the monomer emission enhanced dramatically with the increase of **DTAB** (Fig. 2a–2b and 2d). The intensity of monomer emission reached its maximum value at the molar ratio of 1:30, which was 156 times more than that of **$FPtNC_3$** solution. Of note was that the

emission quantum yield was up to 34% and much higher than that of **FPtNC$_3$** solution (2%). It was also superior to the previously reported FPt1 emitter[5]. In contrast with the monomer emission, the excimer emission showed a comparative decrease in intensity (Fig. 2b), which indicated that the monomer was isolated by **DATB** and the formation of excimer was interrupted partially. Upon successive addition of **DATB**, the intensity of monomer emission started to decrease dramatically (Fig. 2c and 2d). When the ratio was 1:100, the intensity of monomer emission was 15 times than that of **FPtNC$_3$** solution. These results indicated that the incorporation of **DTAB** made **FPtNC$_3$** monomer isolated and thus prevented the formation of excimer. As a result, the energy transfer of monomer became impossible and the monomer emission enhanced efficiently. The same tendency has been confirmed by UV-vis absorbance spectra (Fig. S12).

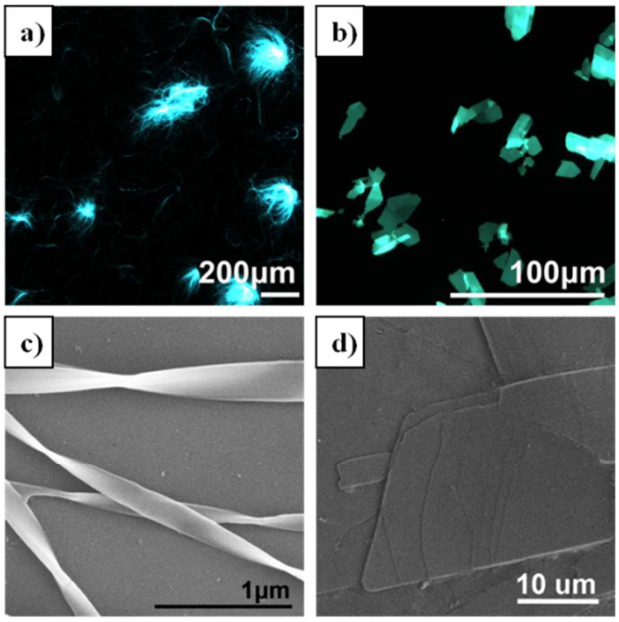

Fig. 3 Fluorescence microscopic images and SEM images of **FPtNC$_3$/DTAB** mixtures at the molar ratio of 1:30 (a, c) and 1:70 (b, d).

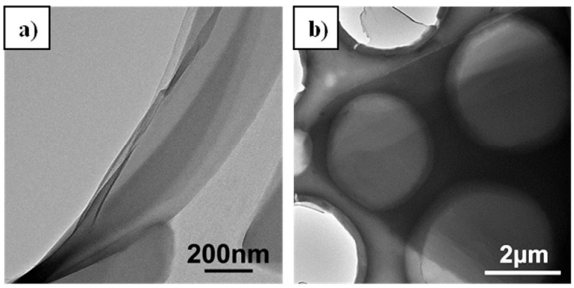

Fig. 4 TEM images of **FPtNC$_3$/DTAB** mixture systems in ribbons (a) and sheets (b).

As above-mentioned description, **FPtNC$_3$** could self-assemble into orange fibers in water due to solvophobic effect. Accordingly, we asked whether the incorporation of **DTAB** would influence the stacking of **FPtNC$_3$** and the **FPtNC$_3$/DTAB** mixtures form new ordered nanostructures. Fluorescence microscope measurement was firstly employed to investigate the aggregates. Fluorescence microscopic images revealed that the **FPtNC$_3$/DTAB** mixtures at the ratio of 1:1 and 1:2 still formed orange fibers (Fig. S14). Upon successive addition of **DTAB**, the orange fibers and bright blue-green ribbons were found at the molar ratio of 1:10 and 1:20 (Fig. S15). The content of blue-green ribbons increased with the increase of DTAB, while the ratio of the orange fibers reduced. This situation agreed well with the luminescence change as shown in Fig. 2. In the following fluorescent micrograph images (Fig. 3a and Fig. S15), only blue-green ribbons were observed at the molar ratio of 1:30 to 1:50. The ribbons were close to the length of several hundred micrometers. Some ribbons aggregated to form star-shaped structures with a diameter of ca. 400 μm, which emitted intense monomer luminescence (Fig. 3a). After the water was evaporated, the ribbons still showed the same blue-green emission (Fig. S16), demonstrating that the solvent evaporation process did not change the luminescent color and aggregate structure formed in water. These results confirmed that the blue-green ribbons were stabilized. In addition, the average thickness of the ribbons were determined to be ca. 55 nm (1:30), 70 nm (1:40) and 85 nm (1:50) and the average width were ca. 300 nm (1:30), 320 nm (1:40) and 370 nm (1:50) through SEM and TEM measurements (Fig. 3c, 4 and S18), respectively. Overall, with the concentration of **DTAB** increasing, the ribbons became wider and thicker. Besides, the random helical ribbons were observed by SEM and TEM images (Fig. S20).

Subsequently, with the increase of **DTAB**, these mixtures aggregated to form bright blue-green sheets at the molar ratio range of 1:60–1:100, as shown in Fig. 3d and Fig. S15. The luminescence and structure did not change after the water was evaporated (Fig. S17), which confirmed that the blue-green sheets were also stabilized. SEM (Fig. 3d) and TEM images (Fig. 5) showed that the sheets were multiple-layer nanostructures. The dimension of sheets was broadening gradually with the increase of **DTAB**. The average dimension was ca. 35 × 15 μm^2 at the molar ratio of 1:60 and 80 × 40 μm^2 at the molar ratio of 1:100, respectively. Interestingly, the interior angle of the sheets was always 60^o.

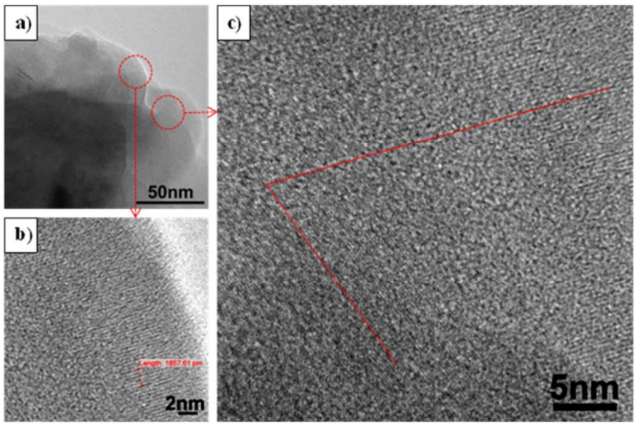

Fig. 5 (a) TEM images of **FPtNC$_3$/DTAB** mixture systems in the sheets. (b,c) the enlarged images of molecule array.

It was noted that TEM images (Fig. 5) revealed the molecule packing style of sheets clearly. The line spacing constant of molecular arrays was found to be 0.37 nm (Fig. 5b), which was consistent with the diameter of trimethylammonium group (calculated 0.35 nm). Considering the similar molecule structures of DTAB and **FPtNC$_3$**, we deduced that the single sheet was consisted of the interdigitated bilayer structure. The crystalline state was formed by surfactants through head to head and tail to tail aggregation, which acquired stable molecular packing by inserting its alkyl chains orderly from both sides of the bilayer. The carbon chains were oriented in parallel to each other and perpendicular to the plane of the layer. The hydrophilic moieties were in the crystalline state, which included a trimethylammonium group and a bromide ion. Moreover, the two molecular arrays between the adjacent bilayers, formed an orientation angle in Fig. 5c. The orientation angle was almost consistent with the interior angle observed in the above microscope images. A possible model was presented in Fig. 6.

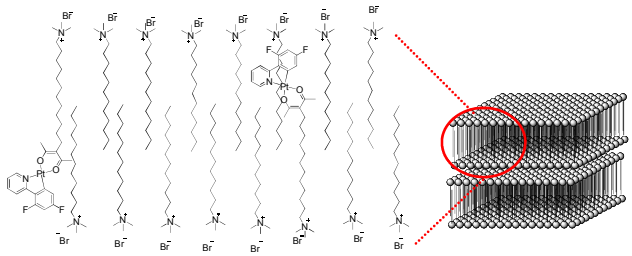

Fig. 6 Schematic representation of a model of the layered aggregation of **FPtNC$_3$/DTAB** mixtures.

In the previous work[4a,4b], the lamellar sheets had been found in some of aqueous cationic systems. Lamellar sheets had also been observed in the sodium dodecyl sulfate (SDS)/DTAB/D_2O system when the overall surfactant concentration is increased.[4e] Previous study[4d] for the **DTAB**/water self-assembly system showed that hydrated crystals **DTAB** occurred at a higher concentrations (>90 wt %) than the total amount of the surfactants range between 78.4% and 85.2% (listed in Table S1). Hence, the formation of sheets was caused by the nature of DTAB mostly and the dual effect of DTAB and **FPtNC$_3$** could not be neglected.

It was apparent that the platinum(II) complex square was limited in the hydrophobic regions of high ordered ribbons and sheets and was isolated by the alkyl chains of DTAB, resulting in the enhancement of monomer emission and the disappearance of excimers. According to the previous literature,[6e] the formation of excimers resulted in the luminescence self-quenching. Hence, the disappearance of excimers led to the efficient monomer emission. Meanwhile, due to the higher percentage of **DTAB** in sheets, **FPtNC$_3$** was diluted by **DTAB** significantly, resulting in a relative weaker emission than that of ribbons.

In summary, we have demonstrated that the incorporation of **DTAB** into the amphiphilic platinum(II)complex **FPtNC$_3$** could tune the spectroscopic and luminescence properties of complex efficiently. Besides this, the aggregate structures of the mixtures transformed from fibres to ribbons then to sheets with the successive addition of **DTAB**. Such approach will provide a facile prepared strategy to develop luminescent materials for potential applications in optoelectronics and solid state lighting.

Notes and references

1. (*a*) K. Kinbara and T. Aida, *Chem. Rev.*, 2005, **105**, 1377; (*b*) L. C. Palmer and S. I. Stupp, *Acc. Chem. Res.*, 2008, **41**, 1674; (*c*) H.-J. Kim, T. Kim and M. Lee, *Acc. Chem. Res.*, 2011, **44**, 72; (d) J. Bae, J.-H. Choi, Y.-S. Yoo, N.-K. Oh, B.-S. Kim and M. Lee, *J. Am. Chem. Soc.* 2005, **127**, 9668; (c) Y. Tidhar, H. Weissman, S. G. Wolf, A. Gulino, and B. Rybtchinski, *Chem. Eur. J.* 2011, **17**, 6068;
2. (a) M.-Y. Yuen, V. A. L. Roy, W. Lu, S. C. F. Kui, G. S. M. Tong, M.-H. So, S. S.-Y. Chui, M. Muccini, J. Q. Ning, S. J. Xu and C.-M. Che, *Angew. Chem. Int. Ed*. 2008, **47**, 9895; (b) K. M.-C. Wong and V. W.-W. Yam, *Acc. Chem. Res.*, 2011, **44**, 424; (c) K. M.-C. Wong, M. M.-Y. Chan and V. W.-W. Yam, *Adv. Mater*. 2014, **26**, 5558; (d) I. Eryazici, C. N. Moorefield and G. R. Newkome, *Chem. Rev.*, 2008, **108**, 1834; (e) S. D. Cummings, *Coord. Chem. Rev.*, 2009, **253**, 449; (f) R. McGuire Jr., M. C. McGuire and D. R. McMillin, *Coord. Chem. Rev.*, 2010, **254**, 2574; (g) J. Kalinowski, V. Fattori, M. Cocchi and J. A. G. Williams, *Coord. Chem. Rev.*, 2011, **255**, 2401; (h) K. M. C. Wong and V. W.-W. Yam, *Acc. Chem. Res.*, 2011, **44**, 424; (i) T. J. Wadas, Q.-M. Wang, Y.-j. Kim, C. Flaschenreim, T. N. Blanton and R. Eisenberg, *J. Am. Chem. Soc.*, 2004, **126**, 16841; (g) L. J. Grove, J. M. Rennekamp, H. Jude and W. B. Connick, *J. Am. Chem. Soc.*, 2004, **126**, 1594; (k) D. R. McMillin and J. J. Moore, *Coord. Chem. Rev.*, 2002, **229**, 113; (l) C. Po, A. Y.-Y. Tam, K. M.-C. Wong and V. W.-W. Yam, *J. Am. Chem. Soc*., 2011, **133**, 12136.
3. (a) L. Zhang, P. Li, X. Liu, L. Du, and E. Wang, *Adv. Mater.* 2007, **19**, 4279; (b) T. Zhang, C. Spitz, M. Antonietti, and C. F. J. Faul, *Chem. Eur. J.* 2005, **11**, 1001; (c) G. Beaune, B. Dubertret, O. Clément, C. Vayssettes, V. Cabuil, and C. Ménager, *Angew. Chem. Int. Ed*. 2007, **46**, 5421; (d) B. C. R. Guillaume, D. Yogev, and J. H. Fendler, *J. Phys. Chem.* 1991, **95**, 7489.
4. (a) K. M. Lusvardi, A. P. Full and E. W. Kaler, *Langmuir*, 1995, **11**, 487; (b) T. Kodama, A. Ohta, K. Toda, T. Katada, T. Asakawa, S. Miyagishi, *Colloid Surf. A*, 2006, **277**, 20; (c) E. W. Kaler, K. L. Herrington, A. K. Murthy, J. A. N. Zasadzinski, *J. Phys. Chem.* 1992, **96**, 6698; (d) Y. Kondo, H. Uchiyama, N. Yoshino, K. Nishiyama, M. Abe, *Langmuir,* 1995, **11**, 2380; (e) M. Bergström and J. S. Pedersen, *Langmuir,* 1998, **14**, 3754; (f) K. M. McGrath, *Langmuir*, 1995, **11**, 1835; (g) E. Rodenas, C. Dolcet, M. Valiente and E. C. Valeront, *Langmuir*, 1994, **10**, 2088; (h) J. Jin, J. Huang and I. Ichinose, *Angew. Chem. Int. Ed.*, 2005, **44**, 4532.
5. (a) J. Brooks, Y. Babayan, S. Lamansky, P. I. Djurovich, I. Tsyba, R. Bau and M. E. Thompson, *Inorg. Chem.*, 2002, **41**, 3055; (b) V. Adamovich, J. Brooks, A. Tamayo, A. M. Alexander, P. I. Djurovich, B. W. D'Andrade, C. Adachi, S. R. Forrest and M. E. Thompson, *New J. Chem.*, 2002, **26**, 1171; (c) E. L. Williams, K. Haavisto, J. Li and G. E.

Jabbour, *Adv. Mater.*, 2007, **19**, 197; (d) X. H. Yang, Z. X. Wang, S. Madakuni, J. Li and G. E. Jabbour, *Adv. Mater.*, 2008, **20**, 2405; (e) A. F. Rausch. L. Murphy, J. A. Gareth Williams and H. Yersin, *Inorg. Chem.*, 2012, **51**, 312.

6. (a) H. Z. Xie , M. W. Liu , Q. Y. Wang , X. H. Zang , C. S. Lee , L. S. Hung , S. T. Lee , P. E. Teng , H. L. Kwong , H. Zheng , C. M. Che, *Adv. Mater.*, 2001, **13**, 1245; (b) Y. Wang, N. Herron, V. V. Grushin, D. LeCloux, V. Petrov, *Appl. Phys. Lett.*, 2001, **79**, 449; (c) B. Maa, P. I. Djurovich, M. E. Thompsona, *Coord. Chem. Rev.*, 2005, **249**, 1501; (d) D. Kim and J. –L. Brédas, *J. Am. Chem. Soc.*, 2009, **131**, 11371; (e) C.-H. Chen, F.-I. Wu, Y.-Y. Tsai and C.-H. Cheng, *Adv. Funct. Mater.*, 2011, **21**, 3150; (f) J. Han, L. Shen, X. Chen and W. Fang, *J. Mater, Chem. C.*, 2013, **1**, 4227.